2007

Electronic Structure of a Metal-Organic Copper Spin-½ Molecule: Bis(4-cyano-2,2,6,6-tetramethyl-3,5-heptanedionato)copper(II)

David Wisbey
University of Nebraska-Lincoln

Danqin Feng
University of Nebraska-Lincoln

Marshall T. Bremer

Camelia N. Borca

Anthony N. Caruso
carusoan@umkc.edu

See next page for additional authors

Wisbey, David; Feng, Danqin; Bremer, Marshall T.; Borca, Camelia N.; Caruso, Anthony N.; Silvernail, Carter M.; Belot, John; Vescovo, Elio; Ranno, Laurent; and Dowben, Peter A., "Electronic Structure of a Metal-Organic Copper Spin-½ Molecule: Bis(4-cyano-2,2,6,6-tetramethyl-3,5-heptanedionato)copper(II)" (2007). *Peter Dowben Publications*. 230.
https://digitalcommons.unl.edu/physicsdowben/230

J|A|C|S
ARTICLES
Published on Web 04/25/2007

Electronic Structure of a Metal−Organic Copper Spin-$^1/_2$ Molecule: Bis(4-cyano-2,2,6,6-tetramethyl-3,5-heptanedionato)copper(II)

David Wisbey,[†] Danqin Feng,[†] Marshall T. Bremer,[‡] Camelia N. Borca[†,§] Anthony N. Caruso,[‡] Carter M. Silvernail,[||,⊥] John Belot,*[,||] Elio Vescovo,[#] Laurent Ranno,[&] and Peter A. Dowben*[,†]

Contribution from the Dept. of Physics and Astronomy and the Nebraska Center for Materials and Nanoscience, University of Nebraska—Lincoln, Lincoln, Nebraska 68588-0111, Center for Nanoscale Science and Engineering, North Dakota State University, 1805 NDSU Research Park Drive, Fargo, North Dakota 58102, Dept. of Chemistry and the Center for Materials Research and Analysis, University of Nebraska—Lincoln, Lincoln, Nebraska 68588-0111, Brookhaven National Laboratory, National Synchrotron Light Source, Upton, New York 11973, and CNRS Laboratoire Louis Neél, 25 avenue des Martyrs BP 166, 38042 Grenoble CEDEX 09, France

Received January 4, 2007; E-mail: jbelot2@unl.edu; pdowben@unl.edu

Abstract: The metal−organic molecule bis(4-cyano-2,2,6,6-tetramethyl-3,5-heptanedionato)copper(II) (Cu(CNdpm)$_2$) ($C_{24}H_{36}N_2O_4Cu$, Cu(II)) is a copper spin-$^1/_2$ system with a magnetic moment of 1.05 ± 0.04 μ_B/molecule, slightly smaller than the 1.215±0.02 μ_B/molecule for the larger size copper spin-$^1/_2$ system $C_{36}H_{48}N_4O_4Cu{\cdot}C_4H_8O$ (bis(4-cyano-2,2,6,6-tetramethyl-3,5-heptanedionato)copper(II) 4,4′-bipyridylethene−THF). There is generally good agreement between photoemission from vapor-deposited thin films of the $C_{24}H_{36}N_2O_4Cu$ on Cu(111) and Co(111) and model calculations. Although this molecule is expected to have a gap between the highest occupied molecular orbital and the lowest unoccupied molecular orbital, the molecule remains surprisingly well screened in the photoemission final state.

Introduction

The interplay between spin and electronic structure is a central issue in the study of metal−organic and organometallic compounds and tends to result in an emphasis of Mn, Fe, Co, and Ni complexes.[1−3] Copper complexes,[3−8] particularly the diketonates, have been known for decades and offer an opportunity to investigate systems dominated by an unpaired spin, generally without the complexity of spin−orbit coupling. The copper complexes are also desirable because the ligands provide a "tunable" spacer length, flexibility, and orbital connectivity between the coordinately labile Cu^{2+} ions.[3,5] Ligand design, and the resulting coordination, is thus a critical component in fabricating extended Cu metal−organic structures, and many chelates are ambidentate (i.e., support secondary interactions).[3,4,9,10] The resulting self-assembled structures often exhibit extended order in three dimensions.[3,9,10] This can be important when either transport or magnetic properties are of interest.[3−6,11] Apart from the heavily investigated copper phthalocyanines,[7] only a few experimental studies of the electronic structure of adsorbed copper complexes have been undertaken.[4,8]

Inorganic precursors were constructed with β-cyano diketones due to their high-symmetry and ability to promote metal acidity and increase dimensionality through electronically coupled secondary (i.e., dative) interactions. Although the

[†] Dept. of Physics and Astronomy and the Nebraska Center for Materials and Nanoscience, University of Nebraska−Lincoln.
[‡] Center for Nanoscale Science and Engineering, North Dakota State University.
[§] Present address: MicroXAS Beamline X05L, Laboratory for Waste Management, Nuclear Energy and Safety Department (NES), Paul Scherrer Institut, CH-5232 Villigen PSI, Switzerland.
[||] Dept. of Chemistry and the Nebraska Center for Materials and Nanoscience, University of Nebraska−Lincoln.
[⊥] Present address: Dept. of Chemistry, L-17, 139 Smith Hall, Univ. of Minnesota, 207 Pleasant St. SE, Minneapolis, MN 55455-0431.
[#] Brookhaven National Laboratory, National Synchrotron Light Source.
[&] CNRS Laboratoire Louis Neél.

(1) Choi, J.; Dowben, P. A. *Surf. Sci.* **2006**, *600*, 2997−3002.
(2) Liu, J.; Xiao, J.; Choi, S.-B.; Jeppson, P.; Jarabek, L.; Losovyj, Y. B.; Caruso, A. N.; Dowben, P. A. *J. Phys. Chem. B* **2006**, *110*, 26180−26184.
(3) Mroziński, J. *Coord. Chem. Rev.* **2005**, *249*, 2535.
(4) Akitsu, T.; Einaga, Y. *Inorg. Chem.* **2006**, *45*, 9826.
(5) Halcrow, M. A. *Dalton Trans.* **2003**, 4375. Falvello, L. R. *J. Chem. Soc., Dalton Trans.* **1997**, 4463.
(6) del Sesto, R. E.; Arif, A. M.; Miller, J. S. *Inorg. Chem.* **2000**, *39*, 4894. Bleaney, B.; Bowers, K. D. *Proc. R. Soc. (London), Ser. A* **1952**, *214*, 451.
(7) Sugiyama, T.; Sasaki, T.; Kera, S.; Ueno, N.; Munakata, T. *Appl. Phys. Lett.* **2006**, *89*, 202116. Ellis, T.; Park, K. T.; Ulrich, M. D.; Hulbert, S. L.; Rowe, J. E. *J. Appl. Phys.* **2006**, *100*, 093515. Gorgoi, M.; Michaelis, W.; Kampen, T. U.; Schlettwein, D.; Zahn, D. R. T. *Appl. Surf. Sci.* **2004**, *234*, 138. Peisert, H.; Knupfer, M.; Schwieger, T.; Auerhammer, J. M.; Golden, M. S.; Fink, J. *J. Appl. Phys.* **2002**, *91*, 4872. Knupfer, M.; Schwieger, T.; Peisert, H.; Fink, J. *Phys. Rev. B* **2004**, *69*, 165210. Lozzi, L.; Santucci, S.; La Rosa, S.; Delley, B.; Picozzi, S. *J. Chem. Phys.* **2004**, *121*, 1883. Auerhammer, J. M.; Knupfer, M.; Peisert, H.; Fink, J. *Surf. Sci.* **2002**, *506*, 333.
(8) Liu, Q.; Yu, H.; Zhang, X.; Zhang, Z. *J. Mol. Struct.* **1999**, *478*, 23.
(9) Silvernail, C. M.; Yap, G.; Sommer, R. D.; Rheingold, A. L.; Day, V. W.; Belot, J. A. *Polyhedron* **2001**, *20*, 3113.
(10) Nieuwenhuyzen, M.; Schobert, R.; Hampel, F.; Hoops, S. *Inorg. Chim. Acta* **2000**, *304*, 118. Turner, S. S.; Collison, D.; Mabbs, F. E.; Halliwell, M. *J. Chem. Soc., Dalton Trans.* **1997**, 1097. Isakova, V. G.; Baidina, I. A.; Morozova, N. B.; Igumenov, I. K. *Polyhedron* **2000**, *19*, 1097.
(11) Real, J. A.; Andres, E.; Munoz, M. C.; Julve, M.; Granier, T.; Bousseksou, A.; Varret, F. *Science* **1995**, *268*, 265.

10.1021/ja069236e CCC: $37.00

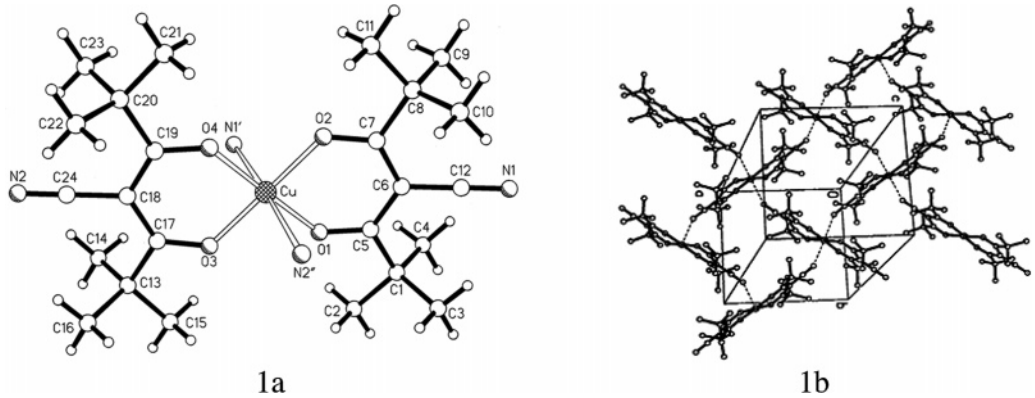

Figure 1. Single-crystal structure, **1a**, and unit cell packing diagram, **1b**, of $Cu(CNdpm)_2$ adapted from ref 9. The immediate coordination geometry about Cu(II) is a tetragonally distorted octahedron exhibiting four short Cu−O equatorial bonds and 2 trans axial Cu−N bonds from adjacent molecules.

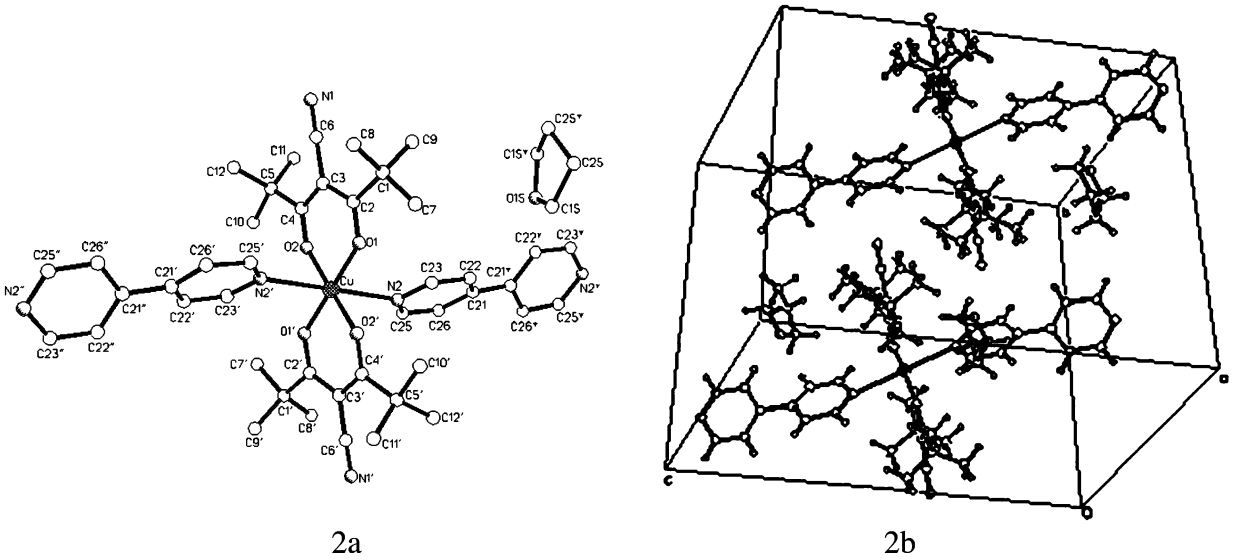

Figure 2. Single-crystal structure, **2a**, and unit cell packing diagram, **2b**, of $C_{36}H_{48}N_4O_4Cu{\cdot}C_4H_8O$ (bis(4-cyano-2,2,6,6-tetramethyl-3,5-heptanedionato)-copper(II) 4,4′-bipyridylethene−THF), i.e., $Cu(CNdpm)_2BPEA$.

β-cyano diketonates have not been heavily investigated,[9,12] we have chosen to study one such species, bis(4-cyano-2,2,6,6-tetramethyl-3,5-heptanedionato)copper(II) ($Cu(CNdpm)_2$), i.e., $C_{24}H_{36}N_2O_4Cu$ (Cu(II)),[9] because of the high vapor pressure (tens of milliTorr) and robust chemical stability that make this metal−organic suitable for electron spectroscopy studies. Nonetheless, this system has an electronic structure that we believe may be representative of an entire class of metal−organic compounds.

Experimental Section

Bis(4-cyano-2,2,6,6-tetramethyl-3,5-heptanedionato)copper(II) ($Cu(CNdpm)_2$) (i.e., $C_{24}H_{36}N_2O_4Cu$ (Cu(II))) was synthesized as described in ref 9 and isolated as large, blue block crystals (>1 cm on an edge) that exhibit high thermal stability (>400 K), decent volatilities, and nearly ideal tetragonal crystal symmetry.[9] The preparation of the related $C_{36}H_{48}N_4O_4Cu{\cdot}C_4H_8O$ (bis(4-cyano-2,2,6,6-tetramethyl-3,5-heptanedionato)copper(II) 4,4′-bipyridylethene−THF) is detailed in the Supporting Information. The solid-state structure of bis(4-cyano-2,2,6,6-tetramethyl-3,5-heptanedionato)copper(II), illustrated in Figure 1, exhibits overall molecular C_{2h} symmetry with average Cu−O bond lengths of 1.92 Å.[9] Bis(4-cyano-2,2,6,6-tetramethyl-3,5-heptanedionato)copper-(II) 4,4′-bipyridylethene−THF is schematically shown in Figure 2. The immediate coordination geometry about Cu(II) is a tetragonally distorted octahedron exhibiting four short Cu−O equatorial bonds and two trans axial Cu−N bonds. While the solid-state packing diagram for ($Cu(CNdpm)_2$) shows independent parallel chains linked by long intermolecular Cu−NC contacts (~2.56 Å) (Figure 1), there is no evidence supporting that molecules adsorbed onto single crystals of Cu(111) or epitaxial Co(111) overlayers adopt a similar structure. Similar intermolecular assemblies have been seen in other copper complexes.[4]

Angle-resolved photoemission spectra (ARPES) were acquired at the U5UA undulator beamline at the National Synchrotron Light Source (NSLS).[13,14] Linearly polarized light from an undulator source was monochromatized using a spherical grating monochromator (SGM) operating in the range 20−150 eV. The ultrahigh vacuum photoemission end-station was equipped with a commercial angle-resolved hemispherical electron energy analyzer (EA125, Omicron GmbH). The

(12) Fackler, P. *J. Chem. Soc.* **1962**, 1957. Angelova, O.; Petrov, G.; Macicek, J. *Acta Crystallogr., Sect. C: Cryst. Struct. Commun.* **1989**, *45*, 710. Angelova, O.; Macicek, J.; Atanasov, M.; Petrov, G. *Inorg. Chem.* **1991**, *30*, 1943. Tsiamis, C.; Tzavellas, L. C.; Stergiou, A.; Anesti, V. *Inorg. Chem.* **1996**, *35*, 4984. Tsiamis, C.; Tzavellas, L. C. *Inorg. Chim. Acta* **1993**, *207*, 179. Venetopoulou, D. K.; Keramidas, K. G.; Voutsas, G. P.; Rentzeperis, P. I.; Goubitz, K.; Tsiamis, C. *Z. Kristallogr.* **1994**, *209*, 170. Thambidurai, S.; Jeyasubramanian, K.; Ramalingam, S. K. *Polyhedron* **1996**, *15*, 4011.

(13) Vescovo, E.; Kim, H.-J.; Dong, Q.-Y.; Nintzel, G.; Carlson, D.; Hulbert, S.; Smith, N. V. *Synchrotron Radiat. News* **1999**, *12*, 10. Johnson, P. D.; Brooks, N. B.; Hulbert, S. L.; Klaffy, R.; Clarke, A.; Sinkovic, B.; Smith, N. V.; Celotta, R.; Kelly, M. H.; Pierce, D. T.; Sheinfein, M. R.; Waclawski, B. J.; Howells. M. R. *Rev. Sci. Instrum.* **1992**, *63*, 1902.

(14) Dowben, P. A.; Waldfried, C.; Komesu, T.; Welipitiya, D.; McAvoy, T.; Vescovo, E. *Chem. Phys. Lett.* **1998**, *283*, 44−50.

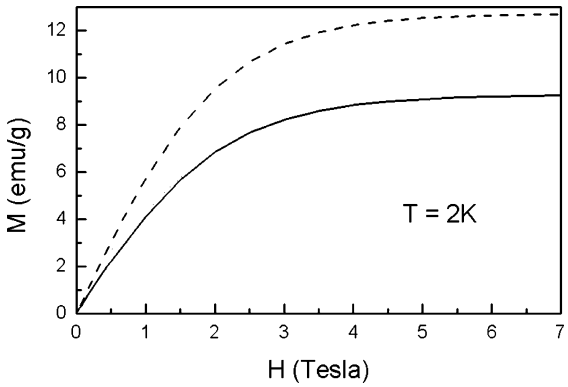

Figure 3. Magnetization curves for $Cu(CNdpm)_2$ (dashed line) and $C_{36}H_{48}N_4O_4Cu{\cdot}C_4H_8O$ (solid line) at 2 K. The saturation magnetization is 1.09 ± 0.01 μ_B moment/formula unit for $Cu(CNdpm)_2$ and 1.215 ± 0.01 μ_B/formula unit for $C_{36}H_{48}N_4O_4Cu{\cdot}C_4H_8O$ in these plots, but there are some sample to sample variations overall.

angular resolution was ~±1°, while the combined energy resolution of the analyzer and the light source was approximately 150 meV or less. The photoemission spectra were taken at a 45° light incidence angle, with the photoelectrons collected normal to the surface. Core-level photoemission was undertaken in a separate ultrahigh vacuum system using a Mg Kα fixed anode source and a Scienta 100 analyzer. All binding energies are referenced to the substrate Fermi level.

A clean Cu(111) surface was prepared by repeated cycles of Ar^+ ion sputtering and annealing of a Cu single crystal. Thick Co(111) films were grown in-situ on the clean Cu(111) substrate, at room temperature, by electron-beam evaporation.[15] As with our studies of the adsorbed metallocenes,[14] the $C_{24}H_{36}N_2O_4Cu$ molecules were deposited on the Cu(111) or Co(111) surfaces at 100 K. Adequate $C_{24}H_{36}N_2O_4Cu$ vapor pressure was obtained by subliming the molecule at a temperature of approximately 80 °C. The choice of cobalt and copper substrates was dictated by the ease of preparation of crystalline epitaxial layers of cobalt grown on Cu(111),[15,16] while both metals have a nominally unpaired spin and a relatively a simple valence band structure. A second substrate (i.e., cobalt), with a lattice constant nearly identical with that of copper was essential so that photoemission could also be undertaken without the complications of copper contributions in resonant photoemission studies.

Magnetization measurements were obtained from the powder both in an extraction magnetometer and using a Quantum Design Physical Properties Measurement System with VSM and ACMS options for dc and ac data collection, at fields of 0 → 7 T and temperatures 2 K → 300 K. The ac susceptibility measurements were completed with H_{dc}= 0 Oe, H_{ac}= 3 Oe, and ν = 9973 Hz. The sample holders were loaded and weighed inside a glovebox with less than 1 ppm H_2O and O_2. The necessary diamagnetic contributions, for the sample holder, were subtracted in the spectra presented.

Metal−Organic Cu Spin-1/2 Molecular Moment and Susceptibility

To establish that the copper ion in $Cu(CNdpm)_2$ is a Pauli spin-1/2 system in the nominally two plus oxidation state, Cu^{2+}, magnetometry was undertaken over a range of temperatures. The $Cu(CNdpm)_2$ molecule, $C_{24}H_{36}N_2O_4Cu$ (Cu(II)), has a magnetic moment of 1.05 ± 0.04 μ_B as derived from the saturation magnetization of $|\mathbf{M}|$ = 11.7−12.7 emu/g obtained

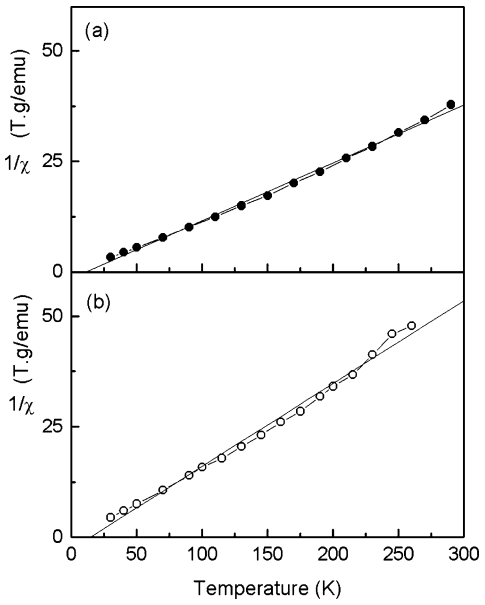

Figure 4. High-field inverse susceptibility, as a function of temperature, for $Cu(CNdpm)_2$ (a) and $C_{36}H_{48}N_4O_4Cu{\cdot}C_4H_8O$ (b). The inverse susceptibility data are derived from the temperature-dependent magnetization and have been fitted to a linear function to obtain the Curie constant (see text).

at 2 K, as illustrated in Figure 3. If the moment is due to the spin moment only, then the spin of $Cu(CNdpm)_2$ is estimated to be $|\mathbf{S}|$ = 0.5−0.544, or close to a spin-1/2 system. The additional contribution to $|\mathbf{S}|$, above $^1/_2$, suggests a ligand or orbital contribution to the spin moment, possibly through the Cu−O bond. Comparison with the larger $C_{36}H_{48}N_4O_4Cu{\cdot}C_4H_8O$ species suggests that this is indeed the case. This is a similar argument as that of Akitsu[4] in which the strong electrostatic flux accompanying weak secondary interactions causes asymmetry of the Jahn−Teller distortion allowing communication between two metal centers by polarization on the Cu $^1/_2$ center mixed into the CN orbital.[4,5]

With the larger ligand, the saturation magnetization of $|\mathbf{M}|$ = 9.25 emu/g indicates that $C_{36}H_{48}N_4O_4Cu{\cdot}C_4H_8O$ has a moment of 1.215 ± 0.02 μ_B/Cu atom, as obtained from the saturation magnetization at 2 K (Figure 3). This suggests that as the moment is larger with the increased ligand size, there is some additional moment "pick-up" from the organic linkers.[4] If the orbital moment is assumed to be entirely suppressed, then the spin moment for $C_{36}H_{48}N_4O_4Cu{\cdot}C_4H_8O$ is $|\mathbf{S}|$= 0.608.

The spin moment can also be estimated from the magnetic susceptibility. In Figure 4, the inverse susceptibility, as a function of temperature, has been plotted for (a) the $Cu(CNdpm)_2$ molecule, $C_{24}H_{36}N_2O_4Cu$ (Cu(II)), and (b) $C_{36}H_{48}N_4O_4Cu{\cdot}C_4H_8O$, respectively. As can be seen, although there are some deviations from strict Curie law dependence, the inverse susceptibility is generally linear except at low temperatures where the high field slope is not well defined (as is common with copper spin-1/2 systems[17]). By fitting the data with a linear function, we obtained the Curie constants *C*, where the values are 0.375 ($cm^3{\cdot}K$)/mol for the $Cu(CNdpm)_2$ and 0.3916 ($cm^3{\cdot}K$)/mol for $C_{36}H_{48}N_4O_4Cu{\cdot}C_4H_8O$. The Curie constant can be used to ascertain the value of the spin magnetic moment that creates the magnetic signal for an insulating paramagnet (no

(15) Chen, Q.; Onellion, M.; Wall, A.; Dowben, P. A. *J. Phys.: Condens. Matter* **1992**, *4*, 7985. Chen, Q.; Onellion, M.; Wall, A. *Thin Solid Films* **1991**, *196*, 103.
(16) Dastoor, P. C.; Allison, W. *Phys. Rev. B* **2001**, *64*, 085414. Dastoor, P. C.; Allison, W. *Surf. Int. Anal.* **1999**, *28*, 65.
(17) Sreedhar, K.; Ganuly, P. *Inorg. Chem.* **1988**, *27*, 2261.

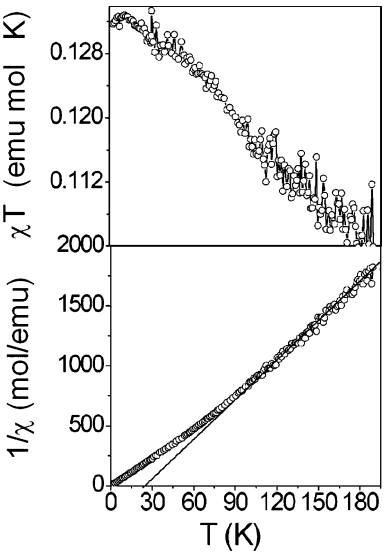

Figure 5. Ac susceptibility as a function of temperature for the Cu(CNdpm)$_2$. The ac susceptibility measurements were done with $H_{dc} = 0$ and $H_{ac} = 3$ Oe. Susceptibility versus temperature (top) shows a negative slope, indicating ferromagnetic exchange. The inverse susceptibility (bottom) versus temperature indicates changes in the magnetic ordering at ~100 K, where a positive Weiss temperature is determined.

doubt an oversimplistic assumption). The susceptibility is defined as

$$\chi = \frac{M}{H} = \frac{Ng^2\mu_B{}^2}{3k_BT} \cdot S(S+1) = \frac{C}{T} \qquad (1)$$

where N is the total number of paramagnetic entities/volume, $g = 2$ is the Landé factor, μ_B is the Bohr magnetron, k_B is the Boltzmann constant, and S is the spin angular momentum quantum number (Curie's Law). The Curie constant C is therefore defined as

$$C = Ng^2\mu_B{}^2S(S+1)/3k_B \qquad (2)$$

Using our values for the Curie constant, we estimate that $|\mathbf{S}| = 0.5$ for Cu(CNdpm)$_2$ and $|\mathbf{S}| = 0.516$ for $C_{36}H_{48}N_4O_4Cu \cdot C_4H_8O$. The discrepancy between the $|\mathbf{S}|$ value for each molecule can be explained by the imperfect application of the Curie law in Figure 3. This again suggests that the larger ligand may add to the total moment of the Cu molecular system. It is not only the ligand but also extramolecular interactions, through ligand interactions, that could affect the net magnetization.

The ac susceptibility is plotted in Figure 5 for Cu(CNdpm)$_2$. The nearly zero slope from 2 to 40 K may indicate a paramagnetic response, while the negative slope in the region of 40 K onward indicates ferromagnetic exchange, at least between adjacent molecules. This signature of ferromagnetic exchange strongly implicates extramolecular interactions between adjacent molecules. Given that the magnetic moments remain widely separated in the crystal (Figure 1), dipolar interactions must be assumed to be very weak, so electronic interactions, possibly via ambidentate interactions, are implicated. We caution that ferromagnetic coupling does not demonstrate overall ferromagnetism. In some respects this extramolecular coupling, for the Cu(CNdpm)$_2$ reported here, is similar to the intramolecular antiferromagnetic coupling reported for $[Cu^{II}L_2][M^{II}(CN)_4] \cdot 2H_2O$ (M(II) = Ni(II) or Pt(II)).[4]

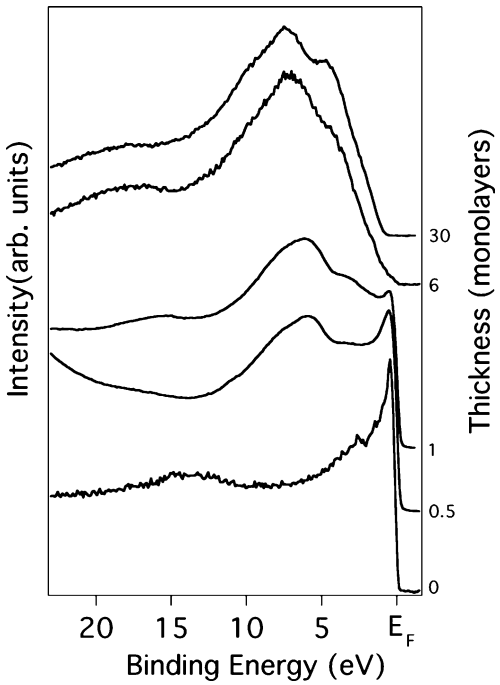

Figure 6. Coverage dependence of Cu(CNdpm)$_2$ adsorbed on an epitaxial Co(111) film at 100 K. The valence band development in photoemission of the Cu(CNdpm)$_2$, with increasing molecular film thickness, on a 20 Å of Co(111) epitaxial film grown on a Cu(111) is shown for a photon energy of 61.5 eV. All photoelectrons are collected along the surface normal (normal emission). The estimated thickness of the Cu(CNdpm)$_2$ films are also indicated.

Electronic Structure of Bis(4-cyano-2,2,6,6-tetramethyl-3,5-heptanedionato)-copper(II) (Cu(CNdpm)$_2$)

The study of the electronic structure of adsorbed Cu(CNdpm)$_2$ was undertaken and exhibited generally good agreement between experiment and expectations. The ultraviolet photoemission spectroscopy (UPS) for adsorbed Cu(CNdpm)$_2$ on clean epitaxial Co(111) films at 100 K (deposited on a Cu(111) single-crystal substrate) is illustrated in Figure 6. Cu(CNdpm)$_2$ molecular orbitals appear at a coverage of only 0.5 molecular monolayers. With increasing Cu(CNdpm)$_2$ coverages, the molecular orbitals increase while the substrate cobalt bands are suppressed. Increasing the Cu(CNdpm)$_2$ molecular film thickness leads to a dramatic reduction of the characteristically sharp cobalt photoemission features near the Fermi edge, whose origin are the Co 3d bands. For very thick coverages of Cu(CNdpm)$_2$, four distinct features emerge in the main peak of the molecule, centered around 6 eV, while another prominent density of states is evident at a binding energy of roughly 18 eV.

As seen in Figure 7, the adsorption of Cu(CNdpm)$_2$ on Cu(111) differs very little from Cu(CNdpm)$_2$ molecular adsorption on Co(111). Although there is considerable solid state and lifetime broadening in the photoemission, the spectra agree with theoretical expectations derived from a semiempirical calculation (PM3, in the unrestricted Hartree Fock method), plotted as the solid line in Figure 7. Figure 7 also shows that for Cu(CNdpm)$_2$ adsorbed on the two different substrates, Cu(111) and Co(111), the same characteristic photoemission features appear at the same binding energies of 4, 8, 11, and 18 eV. The very simplistic calculated representation of the density of states is based on the ground-state molecular orbitals for a single Cu(CNdpm)$_2$

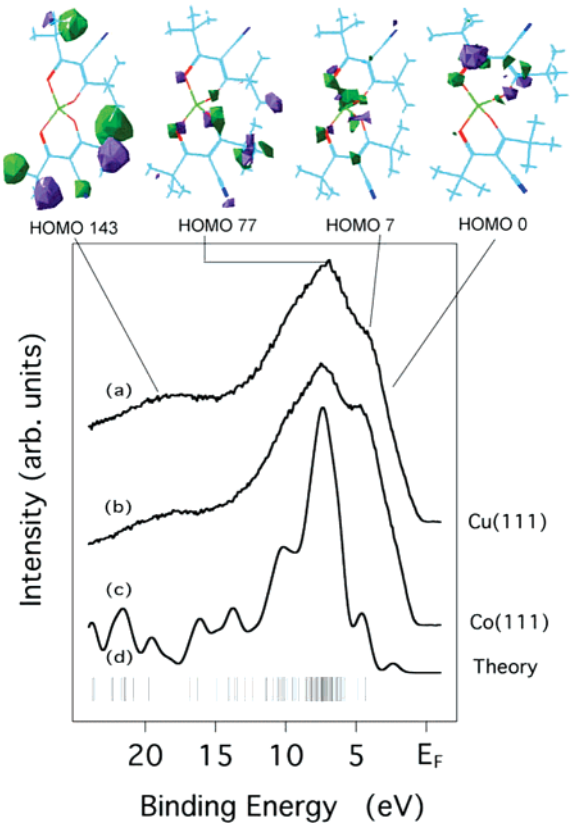

Figure 7. Comparison between $Cu(CNdpm)_2$ adsorbed on (a) Cu(111) and (b) Co(111) at 100 K and (c) the expected density of states. Vertical bars (d) indicate the eigen values for the molecular orbitals. Selected molecular orbitals are schematically shown at the top. The experimental conditions are the same as in Figure 4.

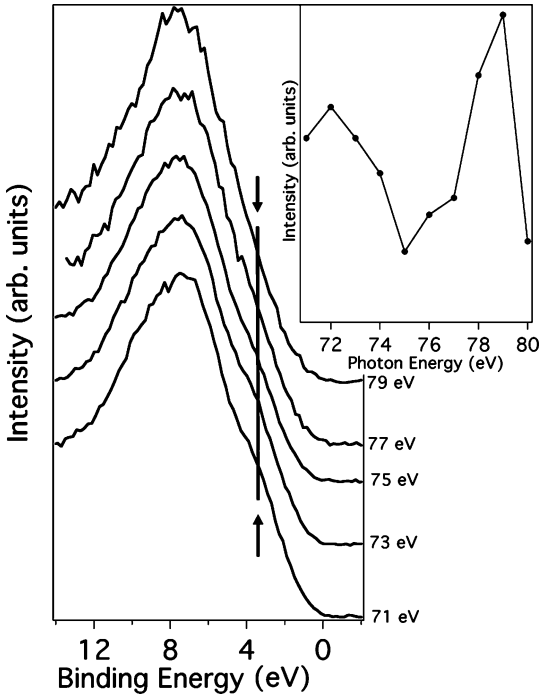

Figure 8. Photon energy dependence of thick $Cu(CNdpm)_2$ film at 100 K. The valence band changes little with photon energy in the region 70−80 eV, although there are enhancements of the feature (the shoulder, indicated by the arrows) at about 5 eV binding energy, at photon energies in the vicinity of 79 eV, i.e., at the Cu $3p_{1/2}$ core threshold. All photoelectrons are collected along the surface normal (normal emission).

molecule, using a 1 eV Gaussian applied to each molecular orbital (the vertical lines below, in Figure 7) without correcting for the substrate, final state, or matrix element effects, as has been done elsewhere.[2,14,18] The width of the photoemission features suggests either substantial lifetime broadening or significant solid-state (extramolecular) effects, such as photohole screening. These angle resolved photoemission spectra are only wave vector dependent (i.e. there is momentum resolution) if the molecular thin film is crystalline. While this might be the case, there is little dependence of the valence band features within 10 eV of the Fermi level, on the photon energy, apart from resonant photoemission effects at the Cu 2p shallow core threshold, as seen in Figure 8.

As indicated in Figure 7, the strong copper weight molecular orbitals contribute to the photoemission features at about 4 eV binding energy. This assignment, suggested by theory, is supported by the resonant photoemission data which shows that this shoulder exhibits a strong resonant enhancement in the region of 79 eV photon energy, or at about the Cu $3p_{1/2}$ threshold at 77 eV binding energy, as indicated in the insert in Figure 8. Indeed the resonant enhancement at 79 eV is suggestive of a super Coster−Kronig resonance with a Fano line shape. Thus some molecular orbitals that contribute to the 4 eV binding energy feature must contain strong Cu weight contributions.

Both the photoemission data and theory indicate that the $Cu(CNdpm)_2$ molecule has a significant HOMO−LUMO gap. The highest occupied molecular orbital (HOMO) for adsorbed $Cu(CNdpm)_2$ appears at an energy of about 2 eV (or more) below the Fermi energy (E_F), in photoemission. Theory suggests a HOMO−LUMO gap of about 7.8 eV, which is not reduced with a larger number of molecules interacting through the bidentate cyanide of adjacent molecules, as indicated in Figure 1.

Molecular thin films of adsorbed $Cu(CNdpm)_2$ are nominally insulating: adsorbed $Cu(CNdpm)_2$ has a large (multi eV) HOMO−LUMO gap and photoemission places the chemical potential well within the gap. In spite of the nominally insulating character of the molecular thin film, the core level photoemission suggests that the copper molecular orbitals of $Cu(CNdpm)_2$ are either delocalized or screened in the photoemission final state. The XPS Cu 2p photoemission for adsorbed $Cu(CNdpm)_2$ and adsorbed $C_{36}H_{48}N_4O_4Cu{\cdot}C_4H_8O$ is shown in Figure 9. The Cu $2p_{3/2}$ binding energies for both $C_{36}H_{48}N_4O_4Cu{\cdot}C_4H_8O$ (at 933 ± 0.2 eV) and $Cu(CNdpm)_2$ (932.8 ± 0.2 eV) are slightly higher than that of copper metal (932.3−932.5 eV [19−21] for the Cu $2p_{3/2}$) but less than the value expected for copper in CuO (933.4,[19] 933.6,[20] 933.7,[21,22] 933.8 eV [23]) or $CuBr_2$ (933.3 eV [19]). Thus, our values for the Cu $2p_{3/2}$ binding energy for both $C_{36}H_{46}N_4O_4Cu{\cdot}C_4H_8O$ (at 933 ± 0.2 eV) and $Cu(CNdpm)_2$ (932.8 ± 0.2 eV) are somewhat smaller than expected, even compared to a similar copper compartmental complex 6,11-

(18) Feng, D.-Q.; Wisbey, D.; Tai, Y.; Losovyj, Ya. B.; Zharnikov, M.; Dowben, P. A. *J. Phys. Chem. B* **2006**, *110*, 1095.

(19) Moulder, J.; Stickle, W.; Sobol, P.; Bomben, K. *Handbook of X-Ray Photoelectron Spectroscopy*; Perkin-Elmer Corp.: Eden Prarie, MN, 1992.
(20) Briggs, D.; Seah, M. P. *Practical surface analysis*, 2nd ed.; John Wiley & Sons: New York, 1993; Vol. 1.
(21) Barr, T. L. *J. Phys. Chem.* **1978**, *82*, 1801−1810.
(22) Barr, T. L. *J. Vac. Sci. Technol., A* **1991**, *9*, 1793−1805. Haemers, G.; Verbist J. J.; Maroie, S. *Appl. Surf. Sci.* **1984**, *17*, 463−476.
(23) Cook, M. G.; Mcintyre, N. S. *Anal. Chem.* **1975**, *47*, 2208−2213. Czanderna, A. W.; King, D. E.; Dake, L. S. *Solid State Sci.* **2000**, *2*, 781−789.

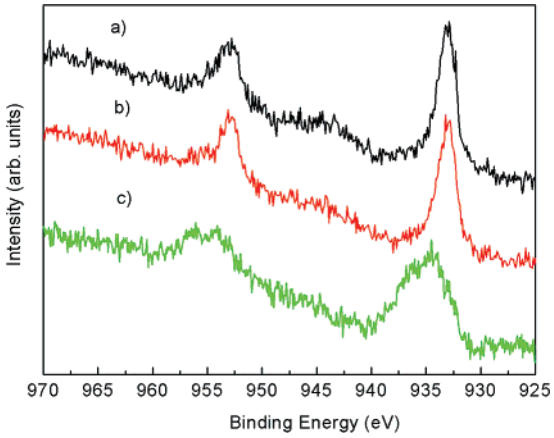

Figure 9. Cu $2p_{1/2}$ and $2p_{3/2}$ X-ray photoelectron spectroscopy for (a) $C_{36}H_{46}N_4O_4Cu{\cdot}C_4H_8O$ and (b) $Cu(CNdpm)_2$, while (c) the decomposition of $Cu(CNdpm)_2$, due to electron irradiation at 50 eV, leads to a species with greater binding energy. All binding energies are referenced to the Fermi level.

dimethyl-7,10 diazahexadeca-5,11-diene-2,4,13,15-tetraene [Cu-(H2daaen)] (934.1 eV [8]), which should have a similar (or even smaller) charge transfer from the Cu metal center. The smaller binding energies for the copper core levels suggest that the photohole is well screened by delocalized electrons (i.e., final state screening[24]), sufficient to overcome the chemical shift, although no corresponding unscreened photon feature can be resolved from our data. A much larger initial state binding energy is also suggested by the valance band photoemission resonance (Figure 8) that occurs at 79 eV photon energy instead of the accepted Cu $3p_{1/2}$ threshold of 77.3 eV; the Cu $2p_{3/2}$ binding energy for $[Cu^{II}L_2][Pt^{II}(CN)_4]{\cdot}2H_2O$ and $[Cu^{II}L_2(H_2O)_2\text{-}(CN_3)_2]$ of 936.9 eV [4] also suggests that the initial state binding energy should be higher.

(24) Ortega, J. E.; Himpsel, F. J.; Li, D.; Dowben, P. A. *Solid State Commun.* **1994**, *91*, 807−811.

By way of comparison, upon decomposition, initiated by either photon or electron irradiation, we find that for the core level binding both $C_{36}H_{48}N_4O_4Cu{\cdot}C_4H_8O$ and $Cu(CNdpm)_2$ exhibit $2p_{3/2}$ binding energies increasing to 935 eV or more, indicative of a copper oxide insulator, with a weakly screened final state. The general absence of charging does suggest that hopping conduction may occur, from the substrate. If screening is the origin for the smaller than expected core level binding energies (for an insulator), both intra- and extramolecular interactions would certainly contribute. The extramolecular interactions would do much to enhance hopping conduction. Both intra- and extramolecular interactions are suggested by the magnetization data, as discussed above.

Conclusions

The metal−organic $Cu(CNdpm)_2$ and $C_{36}H_{48}N_4O_4Cu{\cdot}C_4H_8O$ species are both spin-1/2 systems, as expected. The additional 5−20% increase in spin moment beyond that of a pure spin-1/2 system is a consequence of the delocalized molecular orbitals. The photoemission and susceptibility data suggest that adsorbed $Cu(CNdpm)_2$ exhibits extramolecular interactions, while preserving a significant HOMO−LUMO gap. These extramolecular interactions may be the origin of short-range ferromagnetic exchange.

Acknowledgment. This work was supported by the National Science Foundation through Grant CHE-0415421 and the NSF "QSPINS" MRSEC (Grant DMR 0213808) and through ND EPSCoR Grant EPS-0447679 as well as the Defense Microelectronics Activity (DMEA) under agreement DMEA 90-02-2-0218.

Supporting Information Available: Preparation of $C_{36}H_{48}N_4O_4\text{-}Cu{\cdot}C_4H_8O$ (bis(4-cyano-2,2,6,6-tetramethyl-3,5-heptanedionato)-copper(II) 4,4′-bipyridylethene−THF). This material is available free of charge via the Internet at http://pubs.acs.org.

JA069236E

Supplementary material to "The Electronic Structure of a Metal-Organic Copper Spin ½ Molecule: Bis(4-cyano-2,2,6,6-tetramethyl-3,5-heptanedionato) copper(II) ($Cu(CNdpm)_2$)"

David Wisbey[1], D.Q. Feng[1], M.T. Bremer[2], C.N. Borca[1#], A.N. Caruso[2], Carter M. Silvernail[3†], John Belot[3], E. Vescovo[4], Laurent Ranno[5] and P.A. Dowben[1]**

1) Dept. of Physics and Astronomy and the Center for Materials Research and Analysis, University of Nebraska-Lincoln, Lincoln, NE 68588-0111

2) Center for Nanoscale Science and Engineering, North Dakota State University, 1805 NDSU Research Park Drive, Fargo, ND 58102

3) Dept. of Chemistry and the Center for Materials Research and Analysis, University of Nebraska, Lincoln, NE 68588-0111

4) Brookhaven National Laboratory, National Synchrotron Light Source, Upton, NY, 11973

5) CNRS Laboratoire Louis Neél, 25 avenue des Martyrs BP 166, 38042 Grenoble CEDEX 09, France

A fuller description of the synthetic procedure for Cu(CNdpm)2 . 4,4'dipyridyl . THF {$C_{36}H_{48}N_4O_4Cu * C_4H_8O$ (bis(4-cyano-2,2,6,6-tetramethyl-3,5-heptanedionato)copper(II) 4,4'-bipyridylethene * THF)} is: in a 14/20, 50 mL, 1-neck round bottom flask was dissolved 0.797mmol of copper(II) b-cyanodiketonate in 35 mL of THF. While stirring, 1 equiv (0.797mmol) of 4,4'-dipyridyl was added in one portion. The flask was fitted with a 14/20 reflux condenser and the reaction heated at reflux for 3 hrs. After this time, the reaction cooled to room temperature and evaporation of THF at ambient temperature resulted in analytically pure green microcrystals. Yield 59% (0.333g); mp 270-273?C (dec.). IR(cm-1, KBr pellets): 2969(m), 2197(m), 1605(s), 1584(s), 1467(w), 1395(w), 1366(w), 1336(s), 1208(m), 1066(w), 861(w), 809(w), 739(w), 666(w), 512(w).